# Overview of Advanced Computer Vision Systems for Skin Lesions Characterization

Ilias Maglogiannis, *Member, IEEE*, and Charalampos N. Doukas, *Student Member, IEEE*

***Abstract*—During the last years, computer-vision-based diagnosis systems have been used in several hospitals and dermatology clinics, aiming mostly at the early detection of skin cancer, and more specifically, the recognition of malignant melanoma tumour. In this paper, we review the state of the art in such systems by first presenting the installation, the visual features used for skin lesion classification, and the methods for defining them. Then, we describe how to extract these features through digital image processing methods, i.e., segmentation, border detection, and color and texture processing, and we present the most prominent techniques for skin lesion classification. The paper reports the statistics and the results of the most important implementations that exist in the literature, while it compares the performance of several classifiers on the specific skin lesion diagnostic problem and discusses the corresponding findings.**

***Index Terms*—Classification methods, computer vision, dermoscopy, melanoma, pattern analysis, skin cancer.**

## I. Introduction

THE INTEREST of the biomedical scientific community for computer-supported skin lesion inspection and characterization has been increased during the last years. Skin cancer is among the most frequent types of cancer and one of the most malignant tumors. Its incidence has increased faster than that of almost all other cancers, and the annual rates have increased on the order of 3%–7% in fair-skinned population in recent decades [1]. Currently, between 2 and 3 million nonmelanoma skin cancers and 132 000 melanoma skin cancers occur globally each year. One in every three cancers diagnosed is a skin cancer, and according to the Skin Cancer Foundation Statistics, one in every five Americans will develop skin cancer in their lifetime [2]. The cutaneous melanoma, which is the most common type of skin cancer, is still incurable. However, when it is diagnosed at early stages, it can be treated and cured without complications. The differentiation of early melanoma from other pigmented skin lesions (e.g., benign neoplasms that simulate melanoma) is not trivial even for experienced dermatologists; in several cases, primary care physicians seem to underestimate melanoma in its early stage [3]. The latter has attracted the interest of many researchers, who have developed systems for automated detection of malignancies in skin lesions. The main design issues for the proper characterization of skin lesions concern the image acquisition, the image processing and analysis, the feature extraction, and the classification methodology. This paper presents an overview of existing systems that address the aforementioned issues. In addition, an evaluation of state-of-the-art classifiers is presented in the context of skin lesion characterization, and performance metrics are discussed as well.

This review paper is organized as follows. Section II provides background information on the pathogenic mechanisms of skin cancer in regards to visual differentiations, while Section III presents the image acquisition and feature extraction methods utilized in the literature. Existing classification systems and their corresponding results are discussed in Sections IV and V. Section VI presents results from the conducted experiments concerning the performance evaluation of different classifiers, and Section VII concludes the paper.

## II. Skin Cancer Background Information

The skin consists of a number of layers with distinct function and distinct optical properties. White light shone onto the skin penetrates superficial skin layers, and while some of it is absorbed, much is remitted back and can be registered by a digital camera. The stratum corneum is a protective layer consisting of keratin-impregnated cells, and it varies considerably in thickness. Apart from scattering the light, it is optically neutral. The epidermis is largely composed of connective tissues. It also contains the melanin-producing cells, the melanocytes, and their product, melanin. Melanin is a pigment that strongly absorbs light in the blue part of the visible and the UV spectrum. In this way, it acts as a filter that protects the deeper layers of the skin from harmful effects of UV radiation. Within the epidermal layer, there is very little scattering, with the small amount that occurs being forward directed. The result is that all light not absorbed by melanin can be considered to pass into the dermis. The dermis is made of collagen fibers, and in contrast to the epidermis, it contains sensors, receptors, blood vessels, and nerve ends (see Fig. 1).

Pigmented skin lesions appear as patches of darker color on the skin. In most cases, the cause is excessive melanin concentration in the skin. In benign lesions (e.g., common nevi), melanin deposits are normally found in the epidermis [see Fig. 3(c)]. In malignant lesions (i.e., melanoma), the melanocytes reproduce melanin at a high, abnormal rate (see Fig. 2). While they and their associated melanin remain in the epidermis, melanoma is termed "*in situ*." At this stage, it is not life threatening, and its optical properties make it conform to those of the normal, highly pigmented skin. When malignant melanocytes have penetrated

Manuscript received December 4, 2007; revised July 23, 2008. First published March 16, 2009; current version published September 2, 2009.

I. Maglogiannis is with the Department of Informatics with Appliances in Biomedicine, University of Central Greece, Lamia 35100, Greece (e-mail: imaglo@ucg.gr).

C. N. Doukas is with the Department of Information and Communication Systems Engineering, University of the Aegean, Samos 83200, Greece (e-mail: doukas@aegean.gr).

Digital Object Identifier 10.1109/TITB.2009.2017529

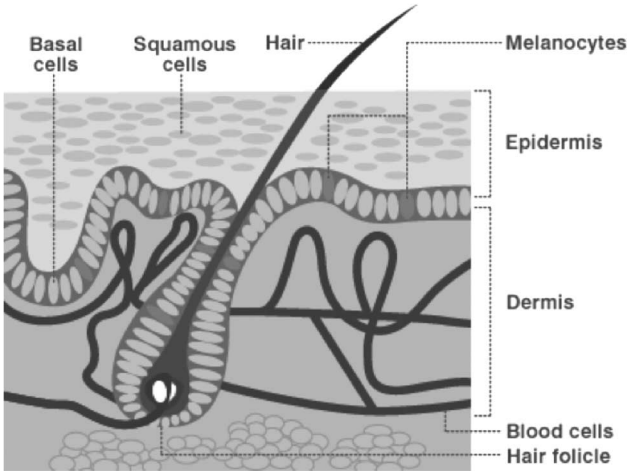


Fig. 1. Normal skin lesions and main components (source: MediceNet).

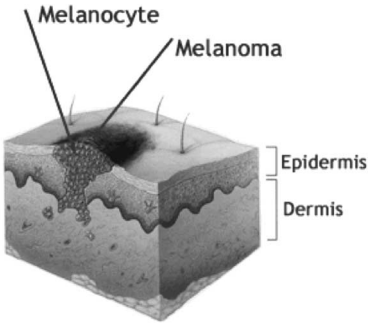


Fig. 2. Illustration of Melanocytes and Melanoma on skin (source: MediceNet).

into the dermis, they leave melanin deposits there, thus changing the nature of skin coloration.

The presence of melanin in the dermis is the most significant sign of melanoma. However, it cannot be used as a sole diagnosis criterion because *in situ* melanomas do not have dermal melanin. Moreover, some benign nevi have dermal deposits, although their spatial patterns tend to be more regular than in melanoma. Other signs, some of which can be indicative of melanoma *in situ*, are thickening of the collagen fibers in the papillary dermis (fibrosis), increased blood supply at the lesion periphery (erythematic reaction), and lack of blood within the lesion in the areas destroyed by cancer. The colors associated with skin, which has melanin deposits in the dermis, normally show characteristic hues not found in any other skin conditions. This provides an important diagnostic cue for a clinician. If the visual approach corroborates a suspicion of skin cancer, histology [4] is needed to make explicit diagnosis. Fig. 3 presents typical example skin lesions of melanoma, dysplastic (benign) nevus, and nondysplastic (common) nevus.

## III. Materials and Methods

In this section, we discuss the discrete modules of an integrated computer-based vision system for the characterization of skin lesions.

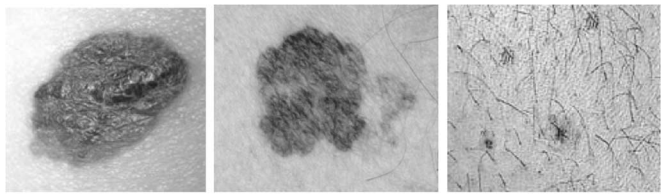


Fig. 3. Illustration of (a) typical melanoma, (b) dysplastic nevus, and (c) nondysplastic (common) nevus.

### A. Image Acquisition Techniques

The first step in expert systems used for skin inspection involves the acquisition of the tissue digital image. The main techniques used for this purpose are the epiluminence microscopy (ELM, or dermoscopy), transmission electron microscopy (TEM), and the image acquisition using still or video cameras. ELM is capable of providing a more detailed inspection of the surface of pigmented skin lesions and renders the epidermis translucent, making many dermal features become visible. TEM, on the other hand, can reveal the typical structure of organization of elastic networks in the dermis, and thus, is mostly used for studying growth and inhibition of melanoma through its liposomes [5]. A recently introduced method of ELM imaging is side-transillumination (transillumination). In this approach, light is directed from a ring around the periphery of a lesion toward its center at an angle of 45°, forming a virtual light source at a focal point about 1 cm below the surface of the skin, thus making the surface and subsurface of the skin translucent. The main advantage of transillumination is its sensitivity to imaging increased blood flow and vascularization and also to viewing the subsurface pigmentation in a nevus. This technique is used by a prototype device, called Nevoscope, which can produce images that have variable amount of transillumination and cross-polarized surface light [6], [7]. The use of commercially available photographic cameras is also quite common in skin lesion inspection systems, particularly for telemedicine purposes [8], [95]. However, the poor resolution in very small skin lesions, i.e., lesions with diameter of less than 0.5 cm, and the variable illumination conditions are not easily handled, and therefore, high-resolution devices with low-distortion lenses have to be used. In addition, the requirement for constant image colors (necessary for image reproducibility) remains unsatisfied, as it requires real time, automated color calibration of the camera, i.e., adjustments and corrections to operate within the dynamic range of the camera and always measure the same color regardless of the lighting conditions. The problem can be addressed by using video cameras [9] that are parameterizable online and can be controlled through software (SW) [10], [11]. In addition to the latter, improper amount of immersion oil or misalignment of the video fields in the captured video frame, due to camera movement, can cause either loss or quality degradation of the skin image. Acquisition time error detection techniques have been developed [11] in an effort to overcome such issues. Computed tomography (CT) images have also been used [12] in order to detect melanomas and track both progress of the

TABLE I
IMAGE ACQUISITION METHODS ALONG WITH THE RESPECTIVE DETECTION GOALS AS RETRIEVED FROM LITERATURE

| Image Acquisition Technique | Detection goal |
|---|---|
| Video RGB Camera | Tumor, crust, hair, scale, shiny ulcer of skin lesions [17], [18], Skin erythema [19], Burn scars [20], Melanoma Recognition [21], [22] |
| Tissue microscopy | Melanoma Recognition [23], [24] |
| Still CCD Camera | Wound Healing [25] |
| Ultraviolet illumination | Melanoma Recognition [26][27] |
| Epiluminescence microscopy (ELM) | Melanoma Recognition [28], [29], [30], [31], [32], [33], [34], [35], [36], [37], [38], [39], [40] [41] |
| Video microscopy | Melanoma Recognition [9], [42], [43] |
| Multi-frequency Electrical Impedance | Melanoma Recognition [15] |
| Raman Spectra | Melanoma Recognition [16] |
| Side- or Epi-transillumination (using Nevoscope) | Melanoma Recognition [6], [44], [45] |

disease and response to treatment. Positron emission tomography (PET) employing fluorodeoxyglucose (FDG) [13] has also been proven to be a highly sensitive and suitable diagnostic method in the staging of various neoplasms, including melanoma, complementing morphologic imaging. FDG uptake has been correlated with proliferation rate, and thus the degree of malignancy of a given tumor. MRI can also be used for tumor delineation [14]. Such methods are utilized mostly for examining the metastatic potential of a skin melanoma and for further assessment. Finally, alternative techniques such multifrequency electrical impedance [15] or Raman spectra [16] have been proposed as potential screening methods. The electrical impedance of a biological material reflects momentary physical properties of the tissue. Raman spectra are obtained by pointing a laser beam at a skin lesion sample. The laser beam excites molecules in the sample, and a scattering effect is observed. These frequency shifts are functions of the type of molecules in the sample; thus, the Raman spectra hold useful information on the molecular structure of the sample. Table I summarizes the most common image acquisition techniques found in literature along with the respective detection goals.

### B. Definition of Features for the Classification of Skin Lesions

In this section, we will examine the features, i.e., the visual cues that are used for skin lesion characterization. Similarly to the traditional visual diagnosis procedure, the computer-based systems look for features and combine them to characterize the lesion as malignant melanoma, dysplastic nevus, or common nevus. The features employed have to be measurable and of high sensitivity, i.e., high correlation of the feature with skin cancer and high probability of true positive response. Furthermore, the features should have high specificity, i.e., high probability of true negative response. Although in the typical classification paradigm both factors are considered important (a tradeoff expressed by maximizing the area under the receiver operating characteristic (ROC) curve), in the case of malignant melanoma detection, the suppression of false negatives (i.e., increase of true positives) is obviously more important.

In the conventional procedure, the following diagnosis methods are mainly used [46]: 1) *ABCD rule* of dermoscopy; 2) *pattern analysis*; 3) *Menzies* method; 4) *seven-point checklist*; and 5) *texture analysis*. The features used for each of these methods are presented in the following.

*1) ABCD Rule:* The ABCD rule investigates the *asymmetry* (A), *border* (B), *color* (C), and *differential structures* (D) of the lesion and defines the basis for a diagnosis by a dermatologist.

*a) Asymmetry:* The lesion is bisected by two axes that are positioned to produce the lowest asymmetry possible in terms of borders, colors, and dermoscopic structures. The *asymmetry* is examined with respect to a point under one or more axes. The asymmetry index is computed first by finding the principal axes of inertia of the tumor shape in the image, and it is obtained by overlapping the two halves of the tumor along the principal axes of inertia and dividing the nonoverlapping area differences of the two halves by the total area of the tumor.

*b) Border:* The lesion is divided into eight pie-piece segments. Then, it is examined if there is a sharp, abrupt cutoff of pigment pattern at the periphery of the lesion or a gradual, indistinct cutoff. Border-based features describing the shape of the lesion are then computed. In order to extract *border information*, image segmentation is performed. It is considered to be a very critical step in the whole process of skin lesion identification and involves the extraction of the region of interest (ROI), which is the lesion and its separation from the healthy skin. Most usual methods are based on thresholding, region growing, and color transformation (e.g., principal components transform, CIELAB color space and spherical coordinates [47], and JSEG algorithm [48]). Additional methods involving artificial intelligence techniques like fuzzy borders [49] and declarative knowledge (melanocytic lesion images segmentation enforcing by spatial-relations-based declarative knowledge) are used for determining skin lesion features. The latter methods are characterized as region approaches, because they are based on different colorization among the malignant regions and the main border. Another category of segmentation techniques is contour approaches using classical edge detectors (e.g., Sobel, Canny, etc.) that produce a collection of edges leaving the selection of the boundary up to the human observer. Hybrid approaches [50] use both color transformation and edge detection techniques, whereas snakes or active contours [51] are considered the prominent state-of-the art technique for border detection. More information regarding border detection as well as a performance comparison of the aforementioned methods can be found in [52] and [53].

The most popular border features are the greatest diameter, the area, the border irregularity, the thinness ratio [54], the circularity index (CIRC) [55], the variance of the distance of the border lesion points from the centroid location [55], and the symmetry distance (SD) [49]. The CIRC is mathematically defined by the following equation:

$$\mathrm{CIRC} = \frac{4A\pi}{p^2} \tag{1}$$

where $A$ is the surface of the examined area and $p$ is its perimeter. SD calculates the average displacement among a number of vertexes as the original shape is transformed into a symmetric shape. The symmetric shape closest to the original shape $P$ is called the symmetry transform (ST) of $P$. The SD of an object is determined by the amount of effort required to transform the original shape into a symmetrical shape, and can be calculated as follows:

$$\mathrm{SD} = \frac{1}{n}\sum_{i=0}^{n-1} \|P_i - \widehat{P}_i\|. \tag{2}$$

Apart from regarding the border as a contour, emphasis is also placed on the features that quantify the transition (swiftness) from the lesion to the skin [42]. Such features are the minimum, maximum, average, and variance responses of the gradient operator applied on the intesity image along the lesion border.

*c) Color:* Color properties inside the lesion are examined, and the number of colors present is determined. They may include light brown, dark brown, black, red (red vascular areas are scored), white (if whiter than the surrounding skin), and slate blue. In addition, color texture might be used for determining the nature of melanocytic skin lesions [56]. Typical color images consist of the three-color channels red, green, and blue (RGB). The *color features* are based on measurements on these color channels or other color channels such as cyan, magenta, yellow (CMY), hue, saturation, value (HSV), Y-luminance, UV (YUV) chrominance components, or various combinations of them, linear or not. Additional color features are the spherical coordinates LAB average and variance responses for pixels within the lesion [17]

$$L = \sqrt{R^2 + G^2 + B^2} \tag{3}$$

$$\text{Angle } A = \cos^{-1}\left[\frac{B}{L}\right] \tag{4}$$

$$\text{Angle } B = \cos^{-1}\left[\frac{R}{L\sin(\text{Angle } A)}\right]. \tag{5}$$

Color variegation may be calculated by measuring minimum, maximum, average, and standard deviations of the selected channel values and color intensity, and by measuring chromatic differences inside the lesion [57], [58]. Another method for computing skin colors based on the normal skin structure model is presented in [4].

*d) Differential structures:* The number of structural components present is determined, i.e., pigment network, dots (scored if three or more are present), globules (scored if two or more are present), structureless areas (counted if larger than 10% of lesion), and streaks (scored if three or more are present).

*2) Pattern Analysis:* The pattern analysis method seeks to identify specific patterns, which may be global (reticular, globular, cobblestone, homogeneous, starburst, parallel, multicomponent, nonspecific) or local (pigment network, dots/globules/moles [59], streaks, blue-whitish veil, regression structures, hypopigmentation, blotches, vascular structures).

*3) Menzies Method:* The Menzies method looks for negative features (symmetry of pattern, presence of a single color) and positive (blue-white veil, multiple brown dots, pseudopods, radial streaming, scar-like depigmentation, peripheral black dots/globules, multiple (five to six) colors, multiple blue/gray dots, broadened network).

*4) Seven-Point Checklist:* The seven-point checklist [60], [61] refers to seven criteria that assess both the chromatic characteristics and the shape and/or texture of the lesion. These criteria are atypical pigment network, blue-whitish veil, atypical vascular pattern, irregular streaks, irregular dots/globules, irregular blotches, and regression structures. Each one is considered to affect the final assessment with a different weight. The dermoscopic image of a melanocytic skin lesion is analyzed in order to evidence the presence of these standard criteria; finally, a score is calculated from this analysis, and if a total score of three or more is given, the lesion is classified as malignant, otherwise it is classified as nevus.

*5) Texture Analysis:* Texture analysis is the attempt to quantify texture notions such as "fine," "rough," and "irregular" and to identify, measure, and utilize the differences between them. Textural features and texture analysis methods can be loosely divided into two categories: statistical and structural. Statistical methods define texture in terms of local gray-level statistics that are constant or slowly varying over a textured region. Different textures can be discriminated by comparing the statistics computed over different subregions. Some of the most common textural features are as follows.

*Neighboring gray-level dependence matrix* (NGLDM) and lattice aperture waveform set (LAWS) are two textural approaches used for analyzing and detecting the pigmented network on skin lesions [62]. *Dissimilarity*, $d$, is a measure related to contrast using linear increase of weights as one moves away from the gray level co-occurrence matrix (GLCM) diagonal. Dissimilarity is calculated as follows:

$$d = \sum_{i,j=0}^{N-1} P_{i,j}\,|i-j| \tag{6}$$

where $i$ is the row number, $j$ is the column number, $N$ is the total number of rows and columns of the GLCM matrix, and

$$P_{i,j} = \frac{V_{i,j}}{\sum_{i,j=0}^{N-1} V_{i,j}} \tag{7}$$

is the normalization equation in which $V_{i,j}$ is the digital number (DN) value of the cell $i, j$ in the image window (i.e., the current gray-scale pixel value).

*Angular second moment* (ASM), which is a measure related to orderliness, where $P_{i,j}$ is used as a weight to itself, is given by

$$\mathrm{ASM} = \sum_{i,j=0}^{N-1} iP_{i,j}^2. \tag{8}$$

*GLCM mean*, $\mu_i$, which differs from the familiar mean equation in the sense that it denotes the frequency of the occurrence of one pixel value in combination with a certain neighbor pixel

value, is given by

$$\mu_i = \sum_{i,j=0}^{N-1} i(P_{i,j}). \tag{9}$$

*GLCM standard deviation*, $\sigma_i$, which gives a measure of the dispersion of the values around the mean, is given by

$$\sigma_i = \sqrt{\sum_{i,j=0}^{N-1} P_{i,j}(i-\mu_i)^2}. \tag{10}$$

The researchers that seek to automatically identify skin lesions exploit the available computational capabilities by searching for many of the features stated before, as well as additional features.

*6) Other Features Utilized:* The *differential structures* as described in the ABCD method, as well as most of the patterns that are used by the pattern analysis, the Menzies method, and the seven-point checklist are very rarely used for automated skin lesion classification, obviously due to their complexity. A novel method presented in [56] uses 3-D pseudoelevated images of skin lesions that reveal additional information regarding the irregularity and inhomogeneity of the examined surface.

Several efforts concern measuring the *kinetics of skin lesions*; e.g., [25] and [63]. The ratio of variances RV in [64] has been defined as

$$\mathrm{RV} = \frac{\mathrm{SD}_{\mathrm{B}^2}}{\mathrm{SD}_{\mathrm{B}^2} + \mathrm{SD}_{\mathrm{I}^2} + \mathrm{SD}_{\mathrm{A}^2}} \tag{11}$$

where standard deviation between days ($\mathrm{SD}_{\mathrm{B}^2}$) is the between day variance of the color variable computed using the mean values at each day of all wound sites and subjects, standard deviation intraday ($\mathrm{SD}_{\mathrm{I}^2}$) is the intraday variance of the color variable estimated from the computations at each day of all wound sites and subjects, and standard deviation analytical ($\mathrm{SD}_{\mathrm{A}^2}$) is the variance of the color variable computed using normal skin sites of all subjects and times.

Finally, wavelet analysis has also been used for decomposing the skin lesion image and utilizing wavelet coefficients for its characterization [41]. A combination of both *ABCD* rules and wavelet coefficients has been shown to improve the classification accuracy by 60% [28]. A distribution of the aforementioned feature categories as used by existing works in literature is illustrated in Fig. 4, whereas Table II presents a more detailed overview of the latter with the corresponding references.

The extraction of the previously described features from digital dermatological images is occasionally hindered by noise caused due to dark hairs surrounding the skin lesion. Techniques relying on the identification of the hair location by utilizing morphological operators and replacing the hair pixels by the nearby nonhair pixels have been developed to deal with this issue. Such an algorithm is presented in [68].

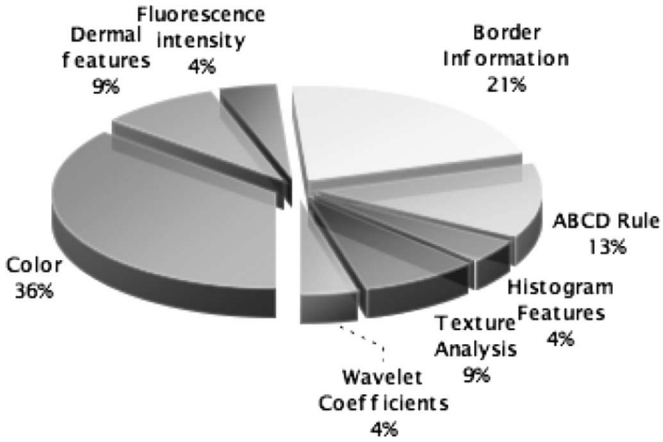


Fig. 4. Illustration of the feature distribution as used by existing systems in literature.

TABLE II
FEATURES UTILIZED FOR SKIN LESION CHARACTERIZATION AND THE RELATED REFERENCES TO EXISTING WORK IN LITERATURE

| Features Category | Special Features | References |
|---|---|---|
| Color | Chromaticity coordinates | [17], [18], [22], [39] |
| | CIE L*a*b* - CIE L*u* υ* color space, | [19], [22], [36] |
| | RGB, HSV and HIS | [21], [25], [29], [65], [30], [33], [34], [35], [66], [37] |
| Dermal Features | Skin Elasticity, Skin impedance, Raman spectra | [20], [15], [16] |
| | Epidermis volume, thickness, dermal epidermal junction ratio, cellular and collagen densities | [23] |
| Fluorescence Intensity | Imax, Imin | [26], [27] |
| Border Information | Border, Boundary shape | [29], [9], [42], [35], [43], [66], [36] |
| | Irregularity, Asymmetry Index | [65], [22] |
| | Correlation coefficient, edge strength and Lesion size. | [6] |
| ABCD Rule | | [44], [28], [31], [67], [43], [38], [58] |
| Histogram Features | Mean value, standard deviation, skewness, kurtosis and entropy of the grey level distribution | [32], [34] |
| Texture Analysis | Entropy, ASM | [45], [35]. [43], [39] |
| Wavelet coefficients | | [28], [41] |

## C. Feature Selection

The success of image recognition depends on the correct selection of the features used for the classification. The latter is a typical optimization problem, which may be resolved with heuristic strategies, greedy or genetic algorithms, other computational intelligence methods [69], or special strategies from statistical pattern recognition [e.g., cross-validation (XVAL), leave-one-out (LOO) method, sequential forward floating selection (SFFS), sequential backward floating selection (SBFS), principal component analysis (PCA), and generalized sequential feature selection (GSFS)] [29]. The use of feature selection

algorithms is motivated by the need for highly precise results, computational reasons, and a peaking phenomenon often observed when classifiers are trained with a limited set of learning samples. If the number of features is increased, the classification rate of the classifiers decreases after a peak [70], [71]. A detailed description of feature selection methodologies may be found in [72].

## IV. Skin Lesion Classification Methods

In this section, the most popular methods for skin lesion classification are examined. The task involves mainly two phases after feature selection, learning and testing [57], which are analyzed in the following paragraphs.

### A. Learning Phase

During the learning phase, typical feature values are extracted from a sequence of digital images representing classified skin lesions. The most classical recognition paradigm is statistical [73]. Covariance matrices are computed for the discriminative measures, usually under the multivariate Gaussian assumption. Parametric discriminant functions are then determined, allowing classification of unknown lesions (discriminant analysis). The major problem of this approach is the need for large learning samples.

Neural networks are networks of interconnected nodes composed of various stages that emulate some of the observed properties of biological nervous systems and draw on the analogies of adaptive biological learning. Learning occurs through learning over a large set of data where the learning algorithm iteratively adjusts the connection weights (synapses) by minimizing a given error function [17], [74].

The support vector machine (SVM) is a popular algorithm for data classification in two classes [75]–[77], [36]. SVMs allow the expansion of the information provided by a learning dataset as a linear combination of a subset of the data in the learning set (support vectors). These vectors locate a hypersurface that separates the input data with a very good degree of generalization. The SVM algorithm is based on learning, testing, and performance evaluation, which are common steps in every learning procedure. Learning involves optimization of a convex cost function where there are no local minima to complicate the learning process. Testing is based on model evaluation using the support vectors to classify a test dataset. Performance evaluation is based on error rate determination as the test dataset size tends to infinity.

The adaptive wavelet-transform-based tree-structure classification (ADWAT) method [44] is a specific skin lesion image classification technique that uses statistical analysis of the feature data to find the threshold values that optimally partitions the image-feature space for classification. A known set of images is decomposed using 2-D wavelet transform, and the channel energies and energy ratios are used as features in the statistical analysis. During the classification phase, the tree structure of the candidate image obtained using the same decomposition algorithm is semantically compared with the tree-structure models of melanoma and dysplastic nevus. A classification variable (CV) is used to rate the tree structure of the candidate image. CV is set to a value of 1 when the main image is decomposed. The value of CV is incremented by one for every additional channel decomposed. When the algorithm decomposes a dysplastic nevus image, only one level of decomposition should occur (channel 0). Thus, for values of CV equal to 1, a candidate image is assigned to the dysplastic nevus class. A value of CV greater than 1 indicates further decomposition of the candidate image, and the image is accordingly assigned to the melanoma class.

### B. Testing Phase

The performance of each classifier is tested using an ideally large set (i.e., over 3000 skin lesion image sets) of manually classified images. A subset of them, e.g., 80% of the images, is used as a learning set, and the other 20% of the samples is used for testing using the trained classifier. The learning and test images are exchanged for all possible combinations to avoid bias in the solution. Most usual classification performance assessment in the context of melanoma detection is the true positive fraction (TPF) indicating the fraction of malignant skin lesions correctly classified as melanoma and the true negative fraction (TNF) indicating the fraction of dysplastic or nonmelanoma lesions correctly classified as nonmelanoma, respectively [7], [44]. A graphical representation of classification performance is the ROC curve, which displays the "tradeoff" between sensitivity (i.e., actual malignant lesions that are correctly identified as such, also known as TPF) and specificity (i.e., the proportion of benign lesions that are correctly identified, also known as TNF) that results from the overlap between the distribution of lesion scores for melanoma and nevi [9], [28], [78]. A good classifier is one with close to 100% sensitivity at a threshold such that high specificity is also obtained. The ROC for such a classifier will plot as a steeply rising curve. When different classifiers are compared, the one whose curve rises fastest should be optimal. If sensitivity and specificity were weighted equally, the greater the area under the ROC curve (AUC), the better the classifier is [79]. An extension of ROC analysis found in literature [40] is the three-way ROC analysis that applies to trichotomous tests. It summarizes the discriminatory power of a trichotomous test in a single value, called the volume under surface (VUS) in analogy to the AUC value for dichotomous tests.

## V. Results From Existing Systems

The development of automated systems for the diagnosis of skin lesions is considered as a significant classification task, which preoccupies many biomedical laboratories and research groups; e.g., [21], [23], [27], [29], [66], [80], and [97]. The results of the most important implementations are summarized in this section. Most of the surveyed systems focus on the detection of malignant melanoma and its discrimination from dysplastic or common nevus. However, there exist systems aiming at the detection of different modalities. These lesions include among others tumor, crust, hair, scale, shiny and ulcer [17], [18], erythema [19], burn scars [20], and wounds [25], [63].

The most common installation type seems to be the video camera, obviously due to the control features that it provides [17], [18]–[21]. The still camera is of use in some installations [25], [63], while infrared or UV illumination (*in situ* or *in vivo*) using appropriate cameras is a popular choice as well [26], [27], [80], [94], [96]. Microscopy (or ELM) installations are applied in the works of [23] and [29] and digital videomicroscopy in [9] and [42].

The most common features that are used for automated lesion characterization are the ones that are associated with color in various color spaces (RGB, HIS, CIELab), e.g, color values in [17], [18], [19], [65], and colorbin (i.e., the percentage of the lesion colored foreground pixels) [65]. Some of them combine features in more than one color spaces for better results, e.g., HIS and RGB in [21], [23], [25], [29] and [63], or RBG and colors peculiar to malignant melanomas [30]. The intensity characteristics are also used in works such as [20], and the ratios of maximum to minimum intensity value are incorporated [27]. Asymmetry and border features are quite common, e.g., [29], [42], and [65], while features based on differential structures are very rare. Some works [7], [31], [58], [67] also rely on the whole ABCD rule for lesion characterization. Shape and color features, like area and elevation, calculated mannually by dermatologists have also been used [65].

The most common classification methods are the statistical and rule-based ones; e.g., [19], [21], [23], [26], [27], [40], [42], [43], [66], and [67]. More advanced techniques such as neural networks are presented in works like [16]–[18], [22], [31], [35], [37], [41], and [65], while the $k$-nearest neighborhood classification scheme is applied in [29]. Evidence theory (upper and lower probabilities induced by multivalued mapping) based on the concept of lower and upper bounds for a set of compatible probability distributions is used in [33] for melanoma detection. Classification and regression trees (CART) [81] analysis has been used in [32]. Finally, the ADWAT method for lesion classification is used in [7] and [44].

The success rates for the methods presented in the literature indicate that the work toward automated classification of lesions and melanoma, in particular, may provide good results. Accuracy rates can vary from 70% [45] to 95% [6], whereas sensitivity can score between 82.5% [27] and 100% [9] and specificity between 63.65% [9] and 91.12% [44], respectively. Fig. 5 displays the distribution of the existing systems per classification method, along with the best performance results for each category of classifiers. Detailed results regarding the performance of the classification methods used in existing systems are presented in Table III. As indicated, SVM seems to achieve higher performance in terms of sensitivity and specificity, folowed by ADWAT and CART algorithms.

It should be noted at this point that the aforementioned results refer mostly to the detection of melanotic lesions against nevus or nondysplastic lesions (i.e., two different classes). Furthermore, these results are not comparable but rather indicative, mainly due to the fact that different images from different cases are used. The classification success rates are not applicable to the methods calculating healing indexes. In order to evaluate the performance of several of the presented classification methods and validate the reported results, a skin lesion characterization experiment has been performed utilizing the most prominent feature extraction, feature selection, and classification methods. The results of the performed evaluation are provided in the following section.

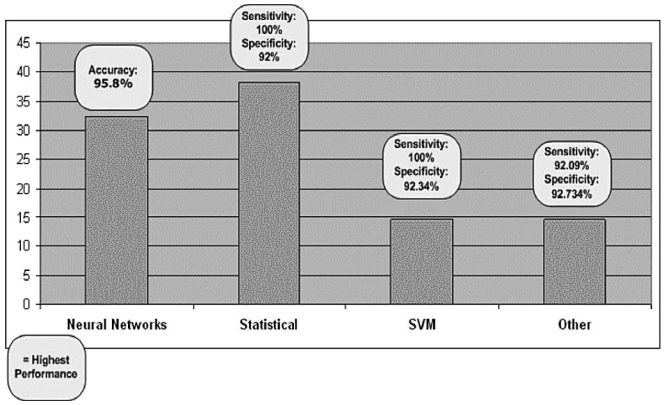


Fig. 5. Distribution and best performance results of existing classification systems. The $Y$-axis represents the percentage of the distribution. The label presents the highest performance reported for the specific category in terms of either accuracy or sensitivity and specificity. "Other" refers to rule-based classification, scoring based on segmentation results, and ADWAT and CART systems.

TABLE III
CLASSIFICATION PERFORMANCE RESULTS FROM EXISTING SYSTEMS

| Classification Method | Performance Results |
|---|---|
| Neural Networks | Accuracy of 85-89% [17][18], Sensitivity of 81%, specificity of 86.7% [65], 90% correlation between manual and automated assessment [31], Accuracy of 80% [22], Accuracy of 94% [35], average AUC 0.7943 [40], average AUC 0.96 [41], Accuracy of 77% [37], Accuracy of 80.5-95.8% [16], Average AUC 0.832 [38] |
| Statistical | 5% deviation from manual diagnosis [21], 5.33% difference from manual diagnosis [23], 77% [26], Sensitivity of 82.5%, specificity of 78.6% [27], Sensitivity of 87%, specificity of 92% [29], Sensitivity of 85.2%, specificity of 72.22% [33], Sensitivity of 85.9%, specificity of 74.1 % [42], Accuracy of 84% [43], Sensitivity of 91%, specificity of 68% [66], average AUC 0.8288 [40], average AUC 0.89 [15], Sensitivity of 100%, specificity of 79-85% [28], Accuracy of 71.8% [39] |
| Ruled-based classification | Detection rate of 26% [30], Sensitivity between 74.2%-86%, specificity between 83.2%-86.3% [67] |
| Scoring system based on segmentation results | Up to 95% success [6] |
| SVM | Sensitivity of 100%, specificity of 63.65% [9], Sensitivity of 92.09%, specificity of 92.734% [45], Sensitivity of 93.3%, specificity of 92.34% [36], average AUC 0.8305 [40], average AUC 0.937 [41] |
| ADWAT | Sensitivity of 93.33%, specificity of 91.12% [44] |
| CART | Sensitivity of 92.09% and a specificity of 92.734% [32] |

TABLE IV
CONFIGURATION PARAMETERS FOR EACH CLASSIFIER

| Classifier (Category) | Input Parameters | Classifier (Category) | Input Parameters |
|---|---|---|---|
| Bayes Networks [82] (Bayes) | Simple Estimator, A: 0.5, search algorithm: hill climbing | RBF Network [82] (Functions – Neural Networks) | num clusters: 2, min stdev: 0.1, ridge: 1.0E-8 |
| NBL [83] (Bayes) | No input | KStar [84] (Lazy) | global Blend: 20 |
| MLR [85] (Functions – Neural Networks) | Ridge estimator:1.0E-8 | LWL [86] (Bayes) | KNN: -1, Classifier: Decision Stump, Linear NN Search |
| SVM [83] (Functions – Neural Networks) | Kernel: RBF, C=1024, g = 0.125 | Classification via Regression [87] (Regression) | Classifier M5P, minNumInstances: 4 |
| Multi-Layer Perceptron [98] (Functions – Neural Networks) | learning rate: 0.3, learning time: 500 validation threshold: 20, num of epochs: 500 | NBTree [88] (Trees) | No input |
| CART [89] (Trees) | heuristic: true, numFold Pruning: 5 | | |

In the case of Bayes Networks numeric estimator precision values are chosen based on analysis of the training data.

TABLE V
EVALUATION RESULTS FOR THE FEATURE SELECTION ALGORITHMS

| Selection Algorithm (Search Algorithm) | CFS (BestFirst) | PCA (Ranker) | GSFS | None |
|---|---|---|---|---|
| Number of Features | 6 | 11 | 18 | 31 |
| Bayes Net | | | | |
| Train model time, validation time | 0.1, 3.1 | 0.13, 3.3 | 0.22,3.5 | 0.33,5.0 |
| Accuracy,TP,FP | 70.41%, 1.0, 0.0 | 66.2%, 0.42,0.04 | 66.2%, 0.4, 0.09 | 68.70%, 0.92, 0.01 |
| SVM | | | | |
| Train model time, validation time | 3.56, 21.2 | 4.42, 35.2 | 5.36, 42.3 | 7.13, 60.0 |
| Accuracy,TP,FP | 73.05%, 1.0, 0.0 | 73.42%, 0.21, 0.02 | 74.11% , 0.3,0.02 | 100%, 1.0,0.0 |
| CART | | | | |
| Train model time, validation time | 3.05, 22.9 | 4.13, 43.4 | 5.89, 69.8 | 7.72, 73 |
| Accuracy, TP, FP | 73.05%, 1.0 , 0.0 | 71.28%, 0.029,0.02 | 71.65% ,0.072, 0.03 | 73.50%, 1.0, 0.0 |

The train model and validation times are in seconds. The feature selection experiments have been performed on a 2.0-GHz Intel CPU with 2 GB RAM and MacOSX operating system.

## VI. PERFORMANCE OF DIFFERENT CLASSIFIERS FOR SKIN LESION CHARACTERIZATION

This section describes the experiments that were conducted in order to evaluate the performance of different classification methods in the context of skin lesion characterization. In order to evaluate the performance of different classification methods, the Weka open-source classification tool has been used available from the University of Waikato [82]. Eleven classifiers have been selected in order to cover all different categories according to the utilized methods (e.g., statistical, rule based, neural networks, regression trees, etc.). The examined classifiers are summarized in Table IV, which presents references for the implementation of each algorithm, the classification category each algorithm belongs to, and the corresponding input parameters, respectively.

### A. Description of Image Dataset

The image dataset used in this study is an extraction of the skin database that exists at the Vienna Hospital, kindly provided by Dr. Ganster. The whole dataset consists of 3639 images, 972 of them are displaying nevus (dysplastic skin lesions), 2598 featuring nondysplastic lesions, and the rest of the images contain malignant melanoma cases. The number of the melanoma images set is not so small considering the fact that malignant melanoma cases in a primordial state are very rare. This dataset is completed by a smaller image dataset containing 26 melanoma and 42 dysplastic nevus cases, captured from patients in the General Hospital of Athens G. Gennimatas with the help of the medical personnel of the Department of Plastic Surgery and Dermatology.

### B. Feature Selection and Utilization

Three types of features are utilized in this study: border features that cover the A and B parts of the ABCD rule of dermatology, colour features (i.e., RGB color plane average and variance responses for pixels within the lesion, intensity, hue, saturation color space average, spherical coordinates LAB average, etc.) that correspond to the C rules, and textural features (i.e., dissimilarity, ASM, GLCM mean, GLCM standard deviation, etc.) that are based on D rules. All the aforementioned 31 utilized features are analyzed in Section III-B. Three feature selection algorithms (i.e., CFS, PCA, and GSFS, as discussed in Section III-C) were evaluated against the total number of features in order to assess both the complexity reduction of the classification models and the accuracy achieved. The classification methods that were used for this experiment were Bayes networks, SVM, and CART. Both image datasets were utilized for learning, meaning that three classes coresponding to the image types were used: melanoma, dysplastic (nevus), and nondysplastic. The selected evaluation metrics were the train model and tenfold validation execution time, the model accuracy, and the true positive rate (TPR) and the false positive rate (FPR) for the classification of the melanoma class. The obtained results are presented in Table V. As indicated by the latter, the proper feature selection results in an important reduction of the complexity: the train model and tenfold XVAL times can be reduced by 60.5% and 69%, respectively, for the case of the CART method, when reducing the number of features from 31 to 6. Concering the performance of the classifiers, the results seem to be controversial. Using feature selection algorithms, the performance

TABLE VI
CLASSIFICATION RESULTS FOR THE CHARACTERIZATION OF MELANOMA AND NEVUS SKIN LESIONS

| | A (%) | RMS | TPR | FPR | AUC |
|---|---|---|---|---|---|
| Bayes Networks | 97.43 | 0.143 | 0.928 | 0.023 | 0.996 |
| NBL | 96.34 | 0.1528 | 0.449 | 0.0 | 0.998 |
| MLR | 100 | 0.0001 | 1.0 | 0.0 | 1.0 |
| SVM | 100 | 0.0 | 1.0 | 0.0 | 1.0 |
| MultiLayer Perceptron | 100 | 0.0084 | 1.0 | 0.0 | 1.0 |
| RBF Network | 98.55 | 0.1072 | 1.0 | 0.015 | 0.994 |
| KStar | 95.38 | 0.2125 | 0.333 | 0.002 | 0.96 |
| LWL | 100 | 0.0 | 1.0 | 0.0 | 1.0 |
| Classification via Regression | 99.71 | 0.0499 | 0.957 | 0.0 | 0.999 |
| NBTree | 99.90 | 0.0239 | 1.0 | 0.001 | 1.0 |
| CART | 100 | 0 | 1.0 | 0.0 | 1.0 |

The TPR and FPR refer to the detection of melanoma class.

TABLE VII
CLASSIFICATION RESULTS FOR THE CHARACTERIZATION OF DYSPLASTIC AND NONDYSPLASTIC SKIN LESIONS

| | A (%) | RMS | TPR | FPR | AUC |
|---|---|---|---|---|---|
| Bayes Networks | 68.94 | 0.4929 | 0.449 | 0.22 | 0.663 |
| NBL | 72.59 | 0.4386 | 0.001 | 0.001 | 0.649 |
| MLR | 74.84 | 0.4169 | 0.252 | 0.065 | 0.725 |
| SVM | 76.08 | 0.4891 | 0.267 | 0.054 | 0.607 |
| MultiLayer Perceptron | 73.29 | 0.4444 | 0.302 | 0.105 | 0.688 |
| RBF Network | 72.14 | 0.436 | 0.121 | 0.053 | 0.644 |
| KStar | 67.93 | 0.5415 | 0.346 | 0.195 | 0.628 |
| LWL | 72.65 | 0.4384 | 0.0 | 0.01 | 0.627 |
| Classification via Regression | 73.80 | 0.4204 | 0.239 | 0.074 | 0.715 |
| NBTree | 72.45 | 0.4439 | 0.321 | 0.124 | 0.672 |
| CART | 72.68 | 0.4418 | 0.174 | 0.065 | 0.602 |

The TPR and FPR refer to the detection of dysplastic class.

of Bayes networks seems to increase in terms of accuracy as well as TPR and FPR. On the contrary, SVM seems to achieve the highest performance when the whole feature set is used, whereas in the case of CART, PCA and GSFS produce lower scores compared to the other two methods. Considering the fact mentioned before, it is clear that feature selection algorithms can reduce complexity but the performance gain is not always positive and highly depends on the classification algorithm.

### C. Performance Metrics and Results

Three different experiments have been conducted according to the number of defined classes that represent the skin lesion types; the first subexperiment concerned the detection of melanoma against nevus, the second one the classification between dysplastic (nevus) and nondysplastic skin lesions, whereas the third one validates the characterization between all three classes (i.e., melanoma, dysplastic, and nondysplastic). The developed classification models were validated using tenfold XVAL. All 31 image features were utilized for the learning and classification process.

In order to compare the performance and effectiveness of each classifier, accuracy (A), rms, TPR, FPR, and AUC have been selected as the indicative metrics. The corresponding results from the three experiments are presented in Tables VI–VIII, respectively.

TABLE VIII
CLASSIFICATION RESULTS FOR THE CHARACTERIZATION OF MELANOTIC, DYSPLASTIC, AND NONDYSPLASTIC SKIN LESIONS

| | A (%) | RMS | TPR | FPR | AUC |
|---|---|---|---|---|---|
| Bayes Networks | 68.70 | 0.4044 | 0.942 | 0.011 | 0.997 |
| NBL | 70.58 | 0.4077 | 1.0 | 0.013 | 0.999 |
| MLR | 75.04 | 0.338 | 0.986 | 0.0 | 1.0 |
| SVM | 77.06 | 0.3911 | 1.0 | 0.0 | 1.0 |
| MultiLayer Perceptron | 75.15 | 0.3536 | 0.957 | 0.0 | 1.0 |
| RBF Network | 72.56 | 0.3561 | 1.0 | 0.004 | 1.0 |
| KStar | 67.24 | 0.4463 | 0.246 | 0.0 | 0.969 |
| LWL | 73.20 | 0.3592 | 1.0 | 0.0 | 1.0 |
| Classification via Regression | 74.44 | 0.3406 | 0.942 | 0.0 | 1.0 |
| NBTree | 71.98 | 0.373 | 0.681 | 0.02 | 0.986 |
| CART | 73.50 | 0.3548 | 1.0 | 0.0 | 1.0 |

The TPR and FPR refer to the detection of melanotic class.

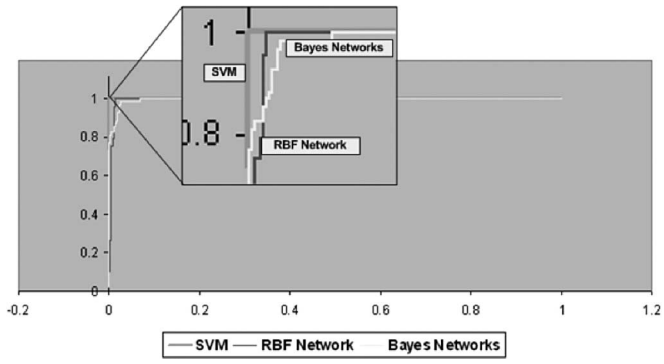


Fig. 6. ROC curves provided by the classification of melanoma against dysplastic skin lesions using SVM, RBF networks, and Bayes networks. Each curve corresponds to a different classifier. $X$-axis represents the FPR, whereas the $Y$-axis presents the TPRs. All the examined classifiers provide high AUC values.

Regarding the first experiment (i.e., distinguishing between melanoma and nevus skin lesions), the majority of the assessed classifiers seem to achieve high accuracy and TPRs in conjunction to low rms and FPRs as well (see Fig. 6). It is also indicated that accuracy itself cannot be considered as an adequate evaluation metric for performance comparison; Bayes networks achieve only 1.09% better accuracy than naïve Bayes mutlinomial (NBL) but in terms of TPR for the detection of melanoma, the difference goes to 51.61%. The latter can be explained due to the inhomogeneity of the learning set (i.e., images acquired with different devices in Vienna and Athens and many fewer images featuring melanoma than the nevus ones). The best performance in terms of accuracy, rms, and TPR and FPR is provided by multinomial logistic regression (MLR), SVM, locally weighted learning (LWL), and CART algorithms.

During the second experiment (i.e., classification between dysplastic (nevi) and nondysplastic skin regions), the majority of the examined classifiers have provided lower detection rates than the previous one: accuracy rates from 68.94 (Kstar) to 76.08 (SVM), whereas TPRs from 0 (LWL) to 0.449 (Bayes networks), respectively. The latter assumption can also be justified by the corresponding ROC curves (Fig. 7) of three of the examined classifiers (i.e., multilayer perceptron, SVM, and Bayes networks) that have achieved the highest performance among all.

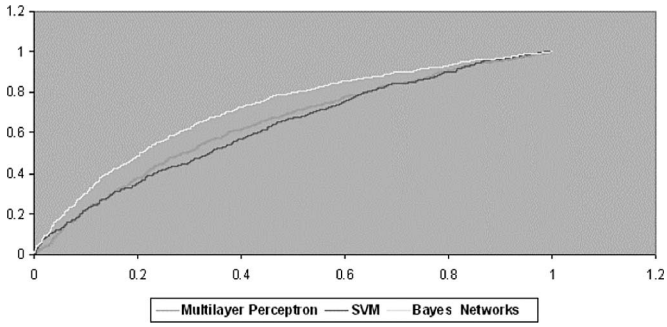


Fig. 7. ROC curves provided by the classification of dysplastic against nondysplastic skin lesions. Each curve corresponds to a different classifier. $X$-axis represents the FPR, whereas the $Y$-axis presents the TPRs.

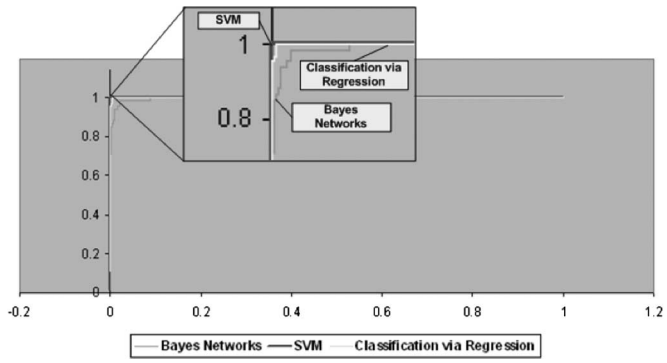


Fig. 8. ROC curves provided by the classification of melanoma against dysplastic and nondysplastic skin lesions, using Bayes networks, SVM, and classification via regression. $X$-axis represents the FPR, whereas the $Y$-axis presents the TPRs.

This difficulty in distinguishing lesions between dysplastic and nondysplastic types is due to the fact that both types have similar features and cannot be easily demarcated even from expert dermatologists by manual assessment [90].

Regarding the detection of melanoma against dysplastic and nondysplastic skin lesions, the majority of the examined classifiers perform satisfactorily. Accuracy ranges from 68.70% (Bayes networks) to 77.06 (SVM), whereas TP from 0.246 (Kstar) to 1.0 (SVM). Fig. 8 compares the performance of three classifiers in terms of AUC. It may be depicted that SMV performs best in this experiment, followed by classification via regression and Bayes networks.

## VII. Discussion and Conclusion

According to the literature [91], [92], it is often difficult to differentiate early melanoma from other benign skin lesions. This task is not trivial even for experienced dermatologists, but it is even more difficult for primary care physicians and general practitioners [3]. On the other hand, the early diagnosis of skin cancer is of severe importance for the outcome of the therapeutic procedure and the basis for reducing mortality rates. Thus, as indicated also by the performed survey, the development of automated characterization systems for skin lesions in clinical settings, aiming mostly at the diagnosis of malignant melanoma, preoccupies several R&D laboratories and medical teams. The most remarkable features of such systems have been surveyed in this paper. These systems employ a variety of methods for the image acquisition and preprocessing, and feature definition and extraction, as well as lesion classification from the extracted features. Regarding the latter, it is clear that the emphasis has been on the assessment of lesion size, shape, color, and texture. However, literature has also indicated that performance can be achieved by combining the most utilized features discussed with alternative features like wavelet coefficients.

Concerning the image acquisition systems, the majority of existing systems use ELM and video microscopy and only a few works use newer techniques like skin impedance and Raman spectra. The quality of ELM images is superior in terms of noise reduction and color fidelity and solves better the shadowing and reflections problems. However, the future trend is to acquire and combine images from alternative spectra and modalities as well (i.e., UV, infrared, and Raman spectra, skin impedance, etc.) in order to improve the overall performance. As far as the classification method is concerned, the SVM algorithm seems to perform better. However, it is actually the selected features that are critical for the performance of the classifier and the learning procedure as well, which has to include the biggest possible variety of cases. It is not clear yet which features are more informative since the surveyed works do not agree in this issue. As the conducted experiment indicated, feature selection methods can improve the classification complexity through minimizing the utilized number of features. However, the performance gain in terms of accuracy depends highly on the selection of a classification method.

All of the surveyed publications include corresponding trials presenting the accuracy and outcomes from the application of such clinical decision support systems (CDSSs) in the assessment of skin pathology. As clinical machine intelligence techniques mature, it seems they can offer increasingly exciting prospects for improving the effectiveness and efficiency of patient care and the development of more reliable CDSS in dermatology. According to a recent review [93], published studies of clinical machine intelligence systems are increasing rapidly, and their quality is improving. The field of automated characterization of skin lesions follows this rule. It seems that the introduction of such diagnostic tools may enhance preventive care in dermatology, facilitating the early diagnosis of skin cancer and monitoring the clinical performance of drugs and therapeutic procedures. Such tools are mostly intended for inexperienced medical personnel that could help them in the diagnosis of skin cancer at early stages. In addition, these decision support systems may be used for their training. When compared to medical experts in the field, even the systems with the best results depict slightly lower performance in terms of accuracy and confidence in diagnosis. However, it is admitted by the physicians that they are very useful in producing quantified results, recording patient follow-ups, and monitoring the therapeutic and healing progress. In any case, the presented systems are not to be used for replacing the physicians, but only to serve as diagnostic adjuncts.

The financial cost of the introduction of a simple CDSS for skin assessment is rather low, roughly estimated less than

3.000 $, calculating the expenses for the appropriate hardware and software for acquisition, store, and classification purposes (software may also be found as open source). However, computer-based vision systems are not yet established in routine clinical practice for skin diagnosis and prognosis, probably because they are not performing convincingly in all cases of the skin pathology. A potential reason for this is that rigorous evaluations of CDSSs are usually more difficult to conduct than evaluations of drug studies, for instance, because clinical settings often preclude complete separation of the intervention and control groups. The studies of patient outcomes also require large numbers of participants and significant budgets, which are not always easy to find, especially from a single institution. Without the existence of such rigorous and well-organized patient outcome studies, the physicians may not be convinced to introduce the use of skin diagnosis tools in the routine practice of healthcare.

It should be, however, noted that the surveyed papers in addition to the evaluation presented in Section VI are quite encouraging for the future. It is our belief that the systems surveyed in this paper have significant evidence to warrant trials with important clinical outcomes. More systematic trials are needed with increased numbers of participants, particularly during the classification phase. This will clarify the issue of selecting the most powerful variables for classification and may also enable even better classification if examination of the differences in results between the alternative methodologies casts light on why misclassifications arise.

Finally, according to our view, the standardization of all steps in the CDSS procedure beginning from the image acquisition (i.e., which devices to be used, which calibration and image corrections should be applied) until the feature extraction (which features to be exploited) and the classification stages (which classifiers to be utilized) is considered essential. This is a difficult task, in which all involving parties, such as medical professionals, computer scientists, academic researchers, and representatives from the medical industry, should participate, regardless of the entity that will coordinate this effort.

## ACKNOWLEDGMENT

The authors wish to thank Dr. H. Ganster for the provision of the skin image dataset captured at the Hospital of Wien and the medical personnel of the Department of Plastic Surgery and Dermatology, General Hospital of Athens G. Gennimatas, for their collaboration.

## REFERENCES

[1] R. Marks, "Epidemiology of melanoma," *Clin. Exp. Dermatol.*, vol. 25, pp. 459–463, 2000.

[2] World Health Organization, Ultraviolet Radiation and the INTERSUN Programme. (2007. Dec.). [Online]. Available: http://www.who.int/uv/faq/skincancer/en/

[3] R. J. Pariser and D. M. Pariser, "Primary care physicians errors in handling cutaneous disorders," *J. Amer. Acad. Dermatol.*, vol. 17, pp. 239–245, 1987.

[4] E. Claridge, S. Cotton, P. Hall, and M. Moncrieff, "From colour to tissue histology: Physics-based interpretation of images of pigmented skin lesions," *Med. Image Anal.*, vol. 7, pp. 489–502, 2003.

[5] T. L. Hwang, W. R. Lee, S. C. Hua, and J. Y. Fang, "Cisplatin encapsulated in phosphatidylethanolamine liposome enhances the in vitro cytotoxicity and in vivo intratumor drug accumulation against melanomas," *J. Dermatol. Sci.*, vol. 46, pp. 11–20, 2007.

[6] G. Zouridakis, M. Doshi, and N. Mullani, "Early diagnosis of skin cancer based on segmentation and measurement of vascularization and pigmentation in nevoscope images," in *Proc. 26th Annu. Int. Conf. IEEE EMBS*, San Francisco, CA, Sep. 1–5, 2004, pp. 1593–1596.

[7] S. V. Patwardhan, S. Dai, and A. P. Dhawan, "Multi-spectral image analysis and classification of melanoma using fuzzy membership based partitions," *Comput. Med. Imag. Graph.*, vol. 29, pp. 287–296, 2005.

[8] M. Loane, H. Gore, R. Corbet, and K. Steele, "Effect of Camera performance on diagnostic accuracy," *J. Telemed. Telecare*, vol. 3, pp. 83–88, 1997.

[9] M. Amico, M. Ferri, and I. Stanganelli, "Qualitative asymmetry measure for melanoma detection," in *Proc. IEEE Int. Symp. Biomed. Imag.: Nano Macro*, Apr. 2004, vol. 2, pp. 1155–1158.

[10] I. Maglogiannis and D. Kosmopoulos, "A system for the acquisition of reproducible digital skin lesion images," *Technol. Healthcare*, vol. 11, pp. 425–441, 2003.

[11] A. Gutenev, V. N. Skladnev, and D. Varvel, "Acquisition-time image quality control in digital dermatoscopy of skin lesions," *Comput. Med. Imag. Graph.*, vol. 25, pp. 495–499, 2001.

[12] J. Solomon, S. Mavinkurve, D. Cox, and R. M. Summers, "Computer-assisted detection of subcutaneous melanomas," *Acad. Radiol.*, vol. 11, no. 6, pp. 678–685, 2004.

[13] C. Pleiss, J. H. Risse, H.-J. Biersack, and H. Bender, "Role of FDG-PET in the assessment of survival prognosis in melanoma," *Cancer Biother. Radiopharm.*, vol. 22, no. 6, pp. 740–747, Dec. 2007.

[14] I. K. Daftari, E. Aghaian, J. M. O'Brien, W. Dillon, and T. L. Phillips, "3D MRI-based tumor delineation of ocular melanoma and its comparison with conventional techniques," *Med. Phys.*, vol. 32, no. 11, pp. 3355–3362, 2005.

[15] P. Åberg, I. Nicander, J. Hansson, P. Geladi, U. Holmgren, and S. Ollmar, "Skin cancer identification using multifrequency electrical impedance—A potential screening tool," *IEEE Trans. Biomed. Eng.*, vol. 51, no. 12, pp. 2097–2102, Dec. 2004.

[16] S. Sigurdsson, P. A. Philipsen, L. K. Hansen, J. Larsen, M. Gniadecka, and H. C. Wulf, "Detection of skin cancer by classification of raman spectra," *IEEE Trans. Biomed. Eng.*, vol. 10, no. 51, pp. 1784–1793, Oct. 2004.

[17] S. E. Umbaugh, R. H. Moss, and W. V. Stoecker, "Applying artificial intelligence to the identification of variegated coloring in skin tumors," *IEEE Eng. Med. Biol. Mag.*, vol. 10, no. 4, pp. 57–62, Dec. 1991.

[18] S. Umbaugh, Y. Wei, and M. Zuke, "Feature extraction in image analysis," *IEEE Eng. Med. Biol.*, vol. 16, no. 4, pp. 62–73, Jul./Aug. 1997.

[19] M. Nischic and C. Forster, "Analysis of skin erythema using true color images," *IEEE Trans. Med. Imag.*, vol. 16, no. 6, pp. 711–716, Dec. 1997.

[20] L. Tsap, D. Goldgof, S. Sarkar, and P. Powers, "Vision-based technique for objective assessment of burn scars," *IEEE Trans. Med. Imag.*, vol. 17, no. 4, pp. 620–633, Aug. 1998.

[21] S. Tomatis, C. Bartol, G. Tragni, B. Farina, and R. Marchesini, "Image analysis in the RGB and HS colour planes for a computer assisted diagnosis of cutaneous pigmented lesions," *Tumori*, vol. 84, pp. 29–32, 1998.

[22] F. Ercal, A. Chawla, W. V. Stoecker, H.-C. Lee, and R. H. Moss, "Neural network diagnosis of malignant melanoma from color images," *IEEE Trans. Biomed. Eng.*, vol. 14, no. 9, pp. 837–845, Sep. 1994.

[23] J. Sanders, B. Goldstein, D. Leotta, and K. Richards, "Image processing techniques for quantitative analysis of skin structures," *Comput. Methods Programs Biomed.*, vol. 59, pp. 167–180, 1999.

[24] H. P. Soyer, J. Smolle, H. Kerl, and H. Stettnre, "Early diagnosis of malignant melanoma by surface microscopy," *Lancet*, vol. 2, p. 803, Oct. 1987.

[25] M. Herbin, F. Bon, A. Venot, F. Jeanlouis, M. Dubertret, L. Dubertret, and G. Strauch, "Assessment of healing kinetics through true color image processing," *IEEE Trans. Med. Imag.*, vol. 12, no. 1, pp. 39–43, Mar. 1993.

[26] A. Bono, S. Tomatis, and C. Bartoli, "The invisible colors of melanoma. A telespectrophotometric diagnostic approach on pigmented skin lesions," *Eur. J. Cancer*, vol. 32A, pp. 727–729, 1996.

[27] B. W. Chwirot, S. Chwirot, J. Redziski, and Z. Michniewicz, "Detection of melanomas by digital imaging of spectrally resolved ultraviolet

light-induced autofluorescence of human skin," *Eur. J. Cancer*, vol. 34, pp. 1730–1734, Oct. 1998.

[28] M. Elbaum, A. W. Kopf, H. S. Rabinovitz, R. Langley, H. Kamino, M. Mihm, A. Sober, G. Peck, A. Bogdan, D. Krusin, M. Greenebaum, S. Keem, M. Oliviero, and S. Wang, "Automatic differentiation of melanoma from melanocytic nevi with multispectral digital dermoscopy: A feasibility study," *J. Amer. Acad. Dermatol*, vol. 44, no. 2, pp. 207–218, 2001.

[29] H. Ganster, P. Pinz, R. Rohrer, E. Wildling, M. Binder, and H. Kittler, "Automated melanoma recognition," *IEEE Trans. Med. Imag.*, vol. 20, no. 3, pp. 233–239, Mar. 2001.

[30] H. Motoyama, T. Tanaka, M. Tanaka, and H. Oka, "Feature of malignant melanoma based on color information," in *Proc. SICE Annu. Conf.*, Sapporo, Japan, Aug. 2004, vol. 1, pp. 230–233.

[31] J. Boldrick, C. Layton, J. Ngyuen, and S. Swtter, "Evaluation of digital dermoscopy in a pigmented lesion clinic: Clinician versus computer assessment of malignancy risk," *J. Amer. Acad. Dermatol.*, vol. 56, no. 3, pp. 417–421, Mar. 2007.

[32] M. Wiltgen, A. Gerger, and J. Smolle, "Tissue counter analysis of benign common nevi and malignant melanoma," *Int. J. Med. Inf.*, vol. 69, pp. 17–28, 2003.

[33] E. Lefevre, O. Colot, P. Vannoorenberghe, and D. de Brucq, "Knowledge modeling methods in the framework of evidence theory: An experimental comparison for melanoma detection," in *Proc. 2000 IEEE Int. Conf. Syst., Man Cybern.*, vol. 4, pp. 2806–2811.

[34] H. Kwasnicka and M. Paradowski, "Melanocytic lesion images segmentation enforcing by spatial relations based declarative knowledge," in *Proc. 5th Int. Conf. Intell. Syst. Des. Appl.*, 2005, pp. 286–291.

[35] P. Rubegni, G. Cevenini, M. Burroni, R. Perotti, G. Dell'Eva, P. Sbano, C. Miracco, P. Luzi, P. Tosi, P. Barbini, and L. Andreassi, "Automated diagnosis of pigmented skin lesions," *Int. J. Cancer*, vol. 101, pp. 576–580, Oct. 2002.

[36] M. E. Celebi, H. A. Kingravi, B. Uddin, H. Iyatomi, Y. A. Aslandogan, W. V. Stoecker, and R. H. Moss, "A methodological approach to the classification of dermoscopy images," *Comput. Med. Imag. Graph.*, vol. 31, pp. 362–373, Mar. 2007.

[37] W. V. Stoecker, K. Gupta, R. J. Stanley, R. H. Moss, and B. Shrestha, "Detection of asymmetric blotches in dermoscopy images of malignant melanoma using relative color," *Skin Res. Technol.*, vol. 11, no. 3, pp. 179–184, Aug. 2005.

[38] K. Hoffmann, T. Gambichler, A. Rick, M. Kreutz, M. Anschuetz, T. Grünendick, A. Orlikov, S. Gehlen, R. Perotti, L. Andreassi, J. Newton Bishop, J.-P. Césarini, T. Fischer, P. J. Frosch, R. Lindskov, R. Mackie, D. Nashan, A. Sommer, M. Neumann, J. P. Ortonne, P. Bahadoran, P. F. Penas, U. Zoras, and P. Altmeyer, "Diagnostic and neural analysis of skin cancer (DANAOS). A multicentre study for collection and computer-aided analysis of data from pigmented skin lesions using digital dermoscopy," *Br. J. Dermatol.*, vol. 149, pp. 801–809, Oct. 2003.

[39] M. Burroni, P. Sbano, G. Cevenini, M. Risulo, G. Dell'eva, P. Barbini, C. Miracco, M. Fimiani, L. Andreassi, and P. Rubegni, "Dysplastic naevus vs. in situ melanoma: Digital dermoscopy analysis," *Br. J. Dermatol.*, vol. 152, pp. 679–684, Apr. 2005.

[40] S. Dreiseitl, L. Ohno-Machado, H. Kittler, S. Vinterbo, H. Billhardt, and M. Binder, "A comparison of machine learning methods for the diagnosis of pigmented skin lesions," *J. Biomed. Inf.*, vol. 34, pp. 28–36, 2001.

[41] G. Surowka and K. Grzesiak-Kopec, "Different learning paradigms for the classification of melanoid skin lesions using wavelets," in *Proc. 29th Annu. Int. Conf. IEEE EMBS*, Aug. 2007, pp. 3136–3139.

[42] C. Grana, G. Pellacani, R. Cucchiara, and S. Seidenari, "A new algorithm for border description of polarized light surface microscopic images of pigmented skin lesions," *IEEE Trans. Med. Imag.*, vol. 22, no. 8, pp. 959–964, Aug. 2003.

[43] A. Blum, H. Luedtke, U. Ellwanger, R. Schwabe, G. Rassner, and C. Garbe, "Digital image analysis for diagnosis of cutaneous melanoma. Development of a highly effective computer algorithm based on analysis of 837 melanocytic lesions," *Br. J. Dermatol.*, vol. 151, no. 5, pp. 1029–1038, Nov. 2004.

[44] S. V. Patwardhan, A. P. Dhawan, and P. A. Relue, "Classification of melanoma using tree structured wavelet transforms," *Comput. Methods Programs Biomed.*, vol. 72, pp. 223–239, 2003.

[45] X. Yuan, Z. Yang, G. Zouridakis, and N. Mullani, "SVM-based texture classification and application to early melanoma detection," *Proc. 28th IEEE EMBS Annu. Int. Conf.*, New York, Aug. 30–Sep. 3, 2006, pp. 4775–4778.

[46] G. Argenziano, H. P. Soyer, S. Chimenti, R. Talamini, R. Corona, F. Sera, M. Binder, L. Cerroni, G. De Rosa, G. Ferrara, R. Hofmann-Wellenhof, M. Landthaler, S. W. Menzies, H. Pehamberger, D. Piccolo, H. S. Rabinovitz, R. Schiffner, S. Staibano, W. Stolz, I. Bartenjev, A. Blum, R. Braun, H. Cabo, P. Carli, V. De Giorgi, M. G. Fleming, J. M. Grichnik, C. M. Grin, A. C. Halpern, R. Johr, B. Katz, R. O. Kenet, H. Kittler, J. Kreusch, J. Malvehy, G. Mazzocchetti, M. Oliviero, F. Ozdemir, K. Peris, R. Perotti, A. Perusquia, M. A. Pizzichetta, S. Puig, B. Rao, P. Rubegni, T. Saida, M. Scalvenzi, S. Seidenari, I. Stanganelli, M. Tanaka, K. Westerhoff, I. H. Wolf, O. Braun-Falco, H. Kerl, T. Nishikawa, K. Wolff, and A. W. Kopf, "Dermoscopy of pigmented skin lesions: Results of a consensus meeting via the Internet," *J. Amer. Acad. Dermatol.*, vol. 48, no. 5, pp. 680–693, 2003.

[47] I. Maglogiannis, C. Caroni, S. Pavlopoulos, and V. Karioti, "Utilizing artificial intelligence for the characterization of dermatological images," in *Proc. 4th Int. Conf. Neural Netw. Exp. Syst. Med. Healthcare (NNESMED)*, 2001, pp. 362–368.

[48] M. E. Celebi, Y. A. Aslandogan, W. V. Stoecker, H. Iyatomi, H. Oka, and X. Chen, "Unsupervised border detection in dermoscopy images," *Skin Res. Technol.*, vol. 13, no. 4, pp. 454–462, 2007.

[49] V. T. Y. Ng, B. Y. M. Fung, and T. K. Lee, "Determining the asymmetry of skin lesion with fuzzy borders," *Comput. Biol. Med.*, vol. 35, pp. 103–120, 2005.

[50] S. E. Umbaugh, R. H. Moss, and W. V. Stoecker, "An automatic color segmentation algorithm with application to identification of skin tumor borders," *Comput. Med. Imag. Graph.*, vol. 16, pp. 227–235, 1992.

[51] K. Taouil and N. B. Romdhane, "Automatic segmentation and classification of skin lesion images," in *Proc. Distrib. Frameworks Multimedia Appl.*, 2006, pp. 1–12.

[52] K. Taouil, B. Romdhane, and M. S. Bouhlel, "A new automatic approach for edge detection of skin lesion image," in *Proc. Inf. Commun. Technol. (ICTTA 2006)*, pp. 212–220.

[53] I. Maglogiannis, "Automated segmentation and registration of dermatological images," *J. Math. Model. Algorithms*, vol. 2, pp. 277–294, 2003.

[54] I. Maglogiannis and E. Zafiropoulos. (2004). Utilizing support vector machines for the characterization of digital medical images. *BMC Med. Inf. Decis. Making.* [Online]. *4(4)*. Available: http://www.biomedcentral.com/content/pdf/1472-6947-4-4.pdf

[55] A. Bono, S. Tomatis, C. Bartoli, G. Tragni, G. Radaelli, A. Maurichi, and R. Marchesini, "The ABCD system of melanoma detection: A spectrophotometric analysis of the asymmetry, border, color, and dimension," *Cancer*, vol. 85, no. 1, pp. 72–77, 1999.

[56] A. G. Manousaki, A. G. Manios, E. I. Tsompanaki, and A. D. Tosca, "Use of color texture in determining the nature of melanocytic skin lesions—A qualitative and quantitative approach," *Comput. Biol. Med.*, vol. 36, pp. 419–427, 2006.

[57] Electronic available information at Skin Oncology Teaching Center. (2007, Dec.) [Online]. Available: http://www.dermoncology.com/

[58] I. Maglogiannis, S. Pavlopoulos, and D. Koutsouris, "An integrated computer supported acquisition, handling and characterization system for pigmented skin lesions in dermatological images," *IEEE Trans. Inf. Technol. Biomed.*, vol. 9, no. 1, pp. 86–98, Mar. 2005.

[59] T. K. Lee, M. S. Atkins, M. A. King, S. Lau, and D. I. McLean, "Counting moles automatically from back images," *IEEE Trans. Biomed. Eng.*, vol. 52, no. 11, pp. 1966–1969, Nov. 2005.

[60] G. Argenziano, G. Fabbrocini, P. Carli, V. De Giorgi, E. Sammarco, and M. Delfino, "Epiluminescence microscopy for the diagnosis of doubtful melanocytic skin lesions. Comparison of the ABCD rule of dermatoscopy and a new 7-point checklist based on pattern analysis," *Arch. Dermatol.*, vol. 134, no. 12, pp. 1563–1570, 1998.

[61] G. Betta, G. Di Leo, G. Fabbrocini, A. Paolillo, and M. Scalvenzi, "Automated application of the "7-point checklist" diagnosis method for skin lesions: Estimation of chromatic and shape parameters," in *Proc. Instrum. Meas. Technol. Conf. (IMTC 2005)*, May, vol. 3, pp. 1818–1822.

[62] M. Anantha, R. H. Moss, and W. V. Stoecker, "Detection of pigmented network in dermatoscopy images using texture analysis," *Comput. Med. Imag. Graph.*, vol. 28, pp. 225–234, 2004.

[63] G. Hansen, E. Sparrow, J. Kokate, K. Leland, and P. Iaizzo, "Wound status evaluation using color image processing," *IEEE Trans. Med. Imag.*, vol. 16, no. 1, pp. 78–86, Feb. 1997.

[64] S. Chin, "The assessment of methods of measurements," *Statist. Med.*, vol. 9, pp. 351–362, 1990.

[65] Z. Zhang, R. H. Moss, and W. V. Stoecker, "Neural networks skin tumor diagnostic system," in *Proc. IEEE Int. Conf. Neural Netw. Signal Process.*, Dec. 2003, vol. 1, pp. 191–192.
[66] S. W. Menzies, L. Bischof, H. Talbot, A. Gutener, M. Avramidis, L. Wong *et al.*, "The performance of SolarScan—An automated dermoscopy image analysis instrument for the diagnosis of primary melanoma," *Arch. Dermatol.*, vol. 141, no. 11, pp. 1388–1396, 2009.
[67] R. J. Stanley, R. H. Moss, W. Van Stoecker, and C. Aggarwal, "A fuzzy-based histogram analysis technique for skin lesion discrimination in dermatology clinical images," *Comput. Med. Imag. Graph.*, vol. 27, pp. 387–396, 2003.
[68] T. Lee, V. Ng, R. Gallagher, A. Coldman, and D. McLean, "DullRazor: A software approach to hair removal from images," *Comput. Biol. Med.*, vol. 27, pp. 533–543, 1997.
[69] H. Handels, Th. Roß, J. Kreusch, H. H. Wolff, and S. J. Pöppl, "Feature selection for optimized skin tumor recognition using genetic algorithms," *Artif. Intell. Med.*, vol. 16, pp. 283–297, 1999.
[70] A. K. Jain, "Advances in statistical pattern recognition," in *Pattern Recognition, Theory and Applications*, P. A. Devijer and J. Kittler, Eds. Berlin, Germany: Springer-Verlag, 1986.
[71] A. K. Jain and W. G. Waller, "On the optimal number of features in the classification of multivariate Gaussian data," *Pattern Recognit*, vol. 10, pp. 365–374, 1978.
[72] M. Kudo and J. Sklansky, "Comparison of algorithms that select features for pattern classifiers," *Pattern Recognit.*, vol. 33, pp. 25–41, 2000.
[73] R. O. Duda and P. E. Hart, *Pattern Classification and Skin Analysis*. New York: Willey, 1973.
[74] A. Durg, W. V. Stoecker, J. P. Vookson, S. E. Umbaugh, and R. H. Moss, "Identification of variegated coloring in skin tumors," *IEEE Eng. Med. Biol. Mag.*, vol. 12, no. 3, pp. 71–75, Sep. 1993.
[75] C. Burges. (2001). A tutorial on support vector machines for pattern recognition [Online]. Available: http://www.kernel-machines.org/
[76] N. Christianini and J. Shawe-Taylor, *An Introduction to Support Vector Machines*. Cambridge, U.K.: Cambridge Univ. Press, 2000.
[77] B. Schölkopf. (2000). Statistical learning and kernel methods [Online]. Available: http://research.Microsoft.com/∼bsc
[78] J. A. Nimunkar, P. A. Dhawan, P. A. Relue, and S. V. Patwardhan, "Wavelet and statistical analysis for melanoma classification," *Progr. Biomed. Opt. Imag.*, vol. 3, no. 3, pp. 1346–1353, 2003.
[79] D. Hagen, "Test characteristics: How good is that test?" *Primary Care*, vol. 22, pp. 213–233, 1995.
[80] W. Lohman and E. Paul, "In situ detection of melanomas by fluorescence measurements," *Naturewissenschaften*, vol. 75, pp. 201–202, 1988.
[81] L. Breiman, J. H. Friedman, R. A. Olshen, and C. J. Stone, *Classification and Regression Trees*. New York/London, U.K.: Chapman & Hall, 1993.
[82] I. H. Witten and E. Frank, *Data Mining: Practical Machine Learning Tools and Techniques*, 2nd ed. San Francisco, CA: Morgan Kaufmann, 2005.
[83] C.-C. Chang and C.-J. Lin. (2001). LIBSVM—A Library for Support Vector Machines [Online]. Available: http://www.csie.ntu.edu.tw/∼cjlin/libsvm/
[84] J. G. Cleary and L. E. Trigg, "K*: An instance-based learner using an entropic distance measure," in *Proc. 12th Int. Conf. Machine Learn.*, 1995, pp. 108–114.
[85] S. Le Cessie and J. C. van Houwelingen, "Ridge estimators in logistic regression," *Appl. Statist.*, vol. 41, no. 1, pp. 191–201, 1992.
[86] E. Frank, M. Hall, and B. Pfahringer, "Locally weighted naive Bayes," in *Proc. 19th Conf. Uncertainty Artif. Intell.*, 2003, pp. 249–256.
[87] E. Frank, Y. Wang, S. Inglis, G. Holmes, and I. H. Witten, "Using model trees for classification," *Mach. Learn.*, vol. 32, no. 1, pp. 63–76, 1998.
[88] R. Kohavi, "Scaling up the accuracy of naive-Bayes classifiers: A decision-tree hybrid," in *Proc. 2nd Int. Conf. Knowl. Discov. Data Mining*, 1996, pp. 202–207.
[89] L. Breiman, J. H. Friedman, R. A. Olshen, and C. J. Stone, *Classification and Regression Trees*. Belmont, CA: Wadsworth, 1984.
[90] G. Altavilla, C. Trabanelli, M. Merlin, A. Caputo, M. Lanfredi, G. Barbanti-Brodano, and A. Corallini, "Morphological, histochemical, immunohistochemical, and ultrastructural characterization of tumors and dysplastic and non neoplastic lesions arising in BK virus/tat transgenic mice," *Amer. J. Pathol.*, vol. 154, pp. 1231–1244, Apr. 1999.
[91] R. B. Mallet, M. E. Fallowfield, M. G. Cook, W. N. Landells, C. A. Holden, and R. A. Marsden, "Are pigmented lesion clinics worthwhile?" *Br. J. Dermatol.*, vol. 129, pp. 689–693, 1993.
[92] M. F. Healsmith, J. F. Bourke, J. E. Osborne, and R. A. C. Graham-Brown, "An evaluation of the revised seven-point checklist for the early diagnosis of cutaneous malignant melanoma," *Br. J. Dermatol.*, vol. 130, pp. 48–50, 1994.
[93] A. X. Garg, N. K. Adhikari, H. McDonald, M. P. Rosas-Arellano, P. J. Devereaux, J. Beyene, J. Sam, and R. B. Haynes, "Effects of computerized clinical decision support systems on practitioner performance and patient outcomes: A systematic review," *J. Amer. Med. Assoc.*, vol. 9, pp. 1223–1238, 2005.
[94] M. Moncrieff, S. Cotton, E. Claridge, and P. Hall, "Spectrophotometric intracutaneous analysis—A new technique for imaging pigmented skin lesions," *Br. J. Dermatol.*, vol. 146, no. 3, pp. 448–457, 2002.
[95] S. Singh, J. H. Stevenson, and D. McGurty, "An evaluation of Polaroid photographic imaging for cutaneous-lesion referrals to an outpatient clinic: A pilot study," *Br. J. Plastic Surg.*, vol. 54, pp. 140–143, 2001.
[96] T. M. Buzug, S. Schumann, L. Pfaffmann, U. Reinhold, and J. Ruhlmann, "Functional infrared imaging for skin-cancer screening," in *Proc. 28th IEEE EMBS Annu. Int. Conf.*, New York City, NY, Aug. 30–Sep. 3, 2006, pp. 2766–2769.
[97] A. Sboner, C. Eccher, E. Blanzieri, P. Bauer, M. Cristofolini, G. Zumiani, and S. Forti, "A multiple classifier system for early melanoma diagnosis," *Artif. Intell. Med.*, vol. 27, pp. 29–44, 2003.
[98] M. Riedmiller, "Advanced supervised learning in multilayer perceptrons—From backpropagation to adaptive learning algorithms," *Comput. Stand. Interfaces*, vol. 16, no. 3, pp. 265–278, Jul. 1994.

**Ilias Maglogiannis** (M'00) received the Diploma in electrical and computer engineering and the Ph.D. degree in biomedical engineering and medical informatics from the National Technical University of Athens (NTUA), Athens, Greece, in 1996 and 2000, respectively.

From 1996 until 2000, he was a Researcher in the Biomedical Engineering Laboratory, NTUA. During 2001, he was a Lecturer in the Department of Information and Communication Systems Engineering, University of the Aegean. Since 2008, he has been an Assistant Professor in the Department of Computer Science and Biomedical Informatics, University of Central Greece, Lamia, Greece. He has been a principal investigator in many European and National Research Programs in biomedical engineering and informatics. He is a reviewer for several scientific journals. He is the author or coauthor of more than 100 papers. His current research interests include biomedical engineering, image processing, computer vision, and multimedia communications.

Dr. Maglogiannis is a member of the International Society for Optical Engineers (SPIE) and the Hellenic Association of Biomedical Engineering. He was a member of program committees of several national and international conferences.

**Charalampos N. Doukas** (S'04) received the Diploma in information and communication systems engineering in 2005 from the University of the Aegean, Samos, Greece, where he is currently working toward the Ph.D. degree.

He is currently an External Researcher at the University of the Aegean. His current research interests include video and image processing of medical data, medical ontologies and semantics, medical data classification, and data transmission over heterogeneous networks.

Mr. Doukas is a member of the Technical Chamber of Greece and the Greek Engineering in Medicine and Biology Society (EMBS). He is currently an External Researcher at the National Hellenic Research Institute, Athens, Greece.